DALTON
FULL PAPER

Metal complexes of 3-carboxyethyl substituted trispyrazolylborates: interactions with the ester carbonyl oxygens

Brian S. Hammes, Xuemei Luo, Balwant S. Chohan, Mary W. Carrano and Carl J. Carrano *

Department of Chemistry and Biochemistry, Southwest Texas State University, San Marcos, TX 78666, USA

Received 25th April 2002, Accepted 25th June 2002
First published as an Advance Article on the web 6th August 2002

The water molecules in complexes $[Tp^{CO_2Et,Me}M(H_2O)_3]^+$ where M = Ni, Co, Mn, or Cu(II) are easily displaced by neutral bidentate ligands, L to produce species of the type $[Tp^{CO_2Et,Me}M(L)H_2O]^+$. Attempted deprotonation of the water molecules in the parent complexes gives rise to rearrangement products for M = Ni, Co and Mn but gives isolable dinuclear hydroxo-bridged species for Zn and Cu. A number of interesting secondary interactions between the H-bond accepting $[Tp^{CO_2Et,Me}]$ group and the other ligands in the metal coordination sphere are revealed by X-ray crystallography. The ester carbonyl C=O stretching frequency of the ligand in the IR is seen to be diagnostic of the type of interaction (*i.e.* nonbonded, H-bonded or weakly complexed, and strongly complexed) between it and the cation, and can be used to provide valuable information in the absence of X-ray crystal structures.

Introduction

"Open" coordination sites, which allow access of substrates and/or cofactors to the catalytically active metal center, are a more or less characteristic feature of the resting state of many metalloenzymes. "Open coordination sites" are however, often not actually vacant, but rather they are occupied by metal-bound water molecules. These labile, metal-bound waters are often important to catalytic function, and metalloproteins containing such sites are widespread. Metal bound water molecules generally provide one or both of two major functions: 1) a ligand that is labile, and thus easily replaceable for inner sphere coordination at the metal by incoming substrates or 2) the metal bound water (or hydroxide) functions as a nucleophile or as a proton donor/acceptor in the actual catalytic reaction. The number of metalloenzymes containing such sites are extremely numerous and include enzymes involved in DNA (phosphodiester), amide, or ester hydrolysis, oxygen activation, isomerizations *etc*. This diversity is well illustrated by the vicinal oxygen chelate (VOC) superfamily.[1] The common thread in the structurally related proteins that make up the VOC superfamily is that they provide a metal coordination environment with two or three "open" (*i.e.* water containing) coordination sites, which promote direct electrophilic participation by the metal ion in catalysis.[1]

Despite the importance of metal aquo complexes, surprisingly few mononuclear well characterized systems of labile metal ions containing adjacent water molecules are known.[2] One of the well established methods to study the reactivity inherent in a particular structure and/or ligand environment of complex molecules such as metalloenzymes is the synthesis, structural characterization, and reactivity studies of small synthetic analogs to these proteins *i.e.* the so called "model compound" approach. This approach has been highly successful in generating spectroscopic, structural and reactivity models for many metalloproteins.[3–7] At the heart of the model compound approach is the design and synthesis of creative ligands to mimic metal ion binding sites. Good models for enzymes of the VOC superfamily could be based on a facially coordinating tripodal chelate which leave two or three sites open at the metal center where water could be bound. However, such water molecules are normally extremely labile, making isolation and characterization of such species problematic. Nature herself often stabilizes such reactive or labile structures through various secondary interactions, the most important of which is hydrogen bonding. While the use of sterically restricted ligands to control the size and shape of metal binding cavities is well established, it has proven more difficult, despite its importance, to incorporate hydrogen bonding into synthetic small molecule binding site analogs.

One of the most successful ligand designs used in metalloenzyme modeling studies has been the tris(pyrazolyl)borate, Tp^R, platform.[3–7] We have recently described a first generation of simple H-bond accepting Tp ligands that simultaneously provides both steric bulk and hydrogen bonding groups directed towards the center of a metal binding cavity.[8] These ligands lead to the stabilization of simple cationic, metal aquo-complexes of the general type $[Tp^{CO_2Et,Me}M(H_2O)_x]^+$ where x = 3 for octahedral favoring Zn(II), Ni(II), Co(II), or Mn(II), and x = 2 for square pyramidal Cu(II). All of these complexes have been crystallographically characterized and the water molecules have been found to be strongly hydrogen bonded to the ester carbonyl moieties.[8] In this report we continue our studies on models for the VOC superfamily by exploring how, or if, the "labile" water molecules can be either deprotonated to yield potentially nucleophilic hydroxo complexes or can undergo substitution with substrate analogs.

Finally, while these ester substituted Tp ligands were originally synthesized with the notion that the carbonyl groups could function as H-bond acceptors to stabilize metal bound water molecules, we show here that the carbonyl oxygens are also well disposed to function as actual metal ligands particularly for the Lewis acidic, high coordination number, lanthanide ions. Several examples of these types of interactions are described.

Results and discussion

Reaction of bidentate ligands with the aquo complexes of Ni and Co

The mechanistic imperative of the VOC superfamily is the displacement of two *cis* coordinated waters at the metal center by bidentate chelating substrates to form an "ES" complex. To model this chemistry we have reacted $[Tp^{CO_2Et,Me}M(H_2O)_3]^+$

 DOI: 10.1039/b204277k

Table 1 Selected bond distances (Å) and angles (°) for [($Tp^{CO_2Me,Me}$)-Ni(Gly)(H_2O)]ClO_4 (**2**), [($Tp^{CO_2Et,Me}$)Co($pz^{CO_2Et,Me}$)(ACN)]ClO_4 (**3a**), and ($Tp^{CO_2Me,Me}$)$_2$Ni (**4**)[a]

	2	3a	4
M(1)–N(1)	2.135(5)	2.112(3)	2.124(2)
M(1)–N(3)	2.199(5)	2.122(3)	2.202(3)
M(1)–N(5)	2.135(6)	2.181(3)	2.124(2)
M(1)–N(7)	2.076(5)	2.176(2)	2.087(2)
M(1)–N(9)		2.126(3)	2.130(3)
M(1)–N(11)		2.099(3)	
M(1)–O(7)	2.095(5)		2.232(2)
M(1)–O(9)	2.035(5)		
N(1)–M(1)–N(3)	87.6(2)	90.47(10)	87.15(9)
N(1)–M(1)–N(5)	89.1(2)	88.20(9)	89.44(9)
N(1)–M(1)–N(7)	95.1(2)	177.04(9)	105.04(10)
N(1)–M(1)–N(9)		89.39(9)	89.49(9)
N(1)–M(1)–N(11)		90.72(10)	
N(1)–M(1)–O(7)	88.3(2)		172.38(9)
N(1)–M(1)–O(9)	175.2(2)		
N(3)–M(1)–N(5)	87.8(2)	87.13(9)	85.27(9)
N(3)–M(1)–N(7)	96.4(2)	90.52(10)	87.40(9)
N(3)–M(1)–N(9)		92.67(9)	176.64(10)
N(3)–M(1)–N(11)		176.24(10)	
N(3)–M(1)–O(7)	172.8(2)		100.47(9)
N(3)–M(1)–O(9)	90.2(2)		
N(5)–M(1)–N(7)	174.1(2)	94.63(9)	163.42(10)
N(5)–M(1)–N(9)		177.59(9)	94.80(10)
N(5)–M(1)–N(11)		89.34(9)	
N(5)–M(1)–O(7)	86.3(2)		90.84(9)
N(5)–M(1)–O(9)	95.1(2)		
N(7)–M(1)–N(9)		87.77(9)	93.39(10)
N(7)–M(1)–N(11)		88.47(9)	
N(7)–M(1)–O(7)	89.8(2)		75.89(9)
N(7)–M(1)–O(9)	80.8(2)		
N(9)–M(1)–N(11)		90.91(9)	
N(9)–M(1)–O(7)			82.90(9)
N(9)–M(1)–O(9)			
N(11)–M(1)–O(7)			
N(11)–M(1)–O(9)			
O(7)–M(1)–O(9)	94.3(2)		

[a] Numbers in parentheses are estimated standard deviations.

complexes of Co(II) and Ni(II) with the amino acids, glycine and methionine methyl ester, as well as with (3-carboxyethyl-5-methyl)pyrazole. As expected the amino acids function as neutral N,O bidentate ligands that coordinate through the carboxylic oxygen and the amino nitrogen and displace two of the three water molecules bound to the metal. The structure of this class of complex is illustrated by that of [$Tp^{CO_2Me,Me}$-Ni(Gly)(H_2O)]ClO_4 **2**. In this structure (Fig. 1, Table 1) the Tp ester functions as a facially coordinating tridentate ligand, and the amino acid as an N,O bidentate with a single remaining water molecule completing the near octahedral coordination of the Ni(II). The only notable deviation from octahedral geometry is the rather acute (81°) O9–Ni1–N7 angle caused by the small bite of the bidentate coordinated glycine. The other coordination angles are all within 6° of the ideal. The Ni–N bonds fall in three distinct groups the shortest being that between the amino nitrogen (N7) and the Ni at 2.076 Å while the Ni–N1 and Ni–N5 bonds (*trans* to the glycine) are longer (av. 2.135 Å) with the Ni–N3 bond (*trans* to the water) the longest at 2.199 Å. One notable feature of this structure is the internal hydrogen bonding interactions between the amine protons and the ester carbonyl oxygens O1 and O3, and those between the water and carbonyl oxygens O3 and O5. The heavy atom–heavy atom distances, which average 2.89(9) Å, and the N–H–O and O–H–O angles averaging 135(14)° are both indicative of a significant H-bonding interaction. Other bond lengths and angles in the structure are unexceptional. One surprising observation however is the fact that the Tp ligand in complex **2** is in the form of its *methyl* ester rather than the *ethyl* ester that was present in the starting material. This change is apparently due to a metal/base catalyzed transesterification that occurs in the presence of methanol as a solvent (used to increase the solubility of the starting material) and appears to be a rather general feature of the chemistry of this class of compound (*vide infra*).

A preliminary structure of [$Tp^{CO_2Me,Me}$Ni(MetOMe)-(H_2O)] with the potentially tridentate methionine methyl ester was also obtained. However, as the thioether sulfur is not bound to the Ni, the side chain is severely disordered, and the overall structure showed no unusual features, it is not reported in detail here.

One feature evident in both structures is the presence of a potentially nucleophilic metal bound water molecule held in a position where it would be capable of engaging in hydrolytic reaction chemistry with the metal bound "substrate". A possible example of this type of reaction chemistry is illustrated by allowing a sample of the perchlorate salt of the Co(II) complex, [$Tp^{CO_2Et,Me}Co(H_2O)_3]^+$, to stand in an acetonitrile solution for several weeks. The crystals that subsequently appeared were not that of the starting aquo complex but rather the pyrazole containing species [$Tp^{CO_2Et,Me}Co(pz^{CO_2Et,Me})$(ACN)]-$ClO_4$, **3a**. EPR spectra show a change from an axially symmetric signal, with features near $g = 8$ and 3.8, characteristic of [$Tp^{CO_2Et,Me}Co(H_2O)_3]^+$ to a rhombic signal in **3a** with features at $g = 6.5$, 3.4 and 2.1. The structure of **3a** (Fig. 2, selected bond lengths and angles are collected in Table 1) shows that a free carboxyethyl pyrazole has displaced two of the waters and is bound in a bidentate fashion through one of the ring nitrogens

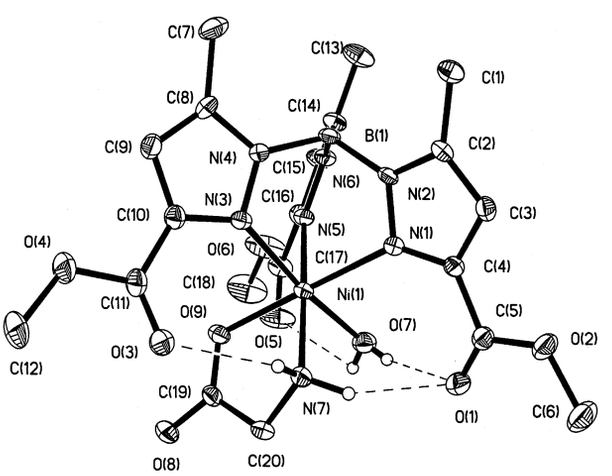

Fig. 1 Thermal ellipsoid diagram of [$Tp^{CO_2Me,Me}$Ni(Gly)(H_2O)] (**2**). The ellipsoids are drawn at the 20% probability level and hydrogens, except those involved in H-bonding, have been removed for clarity.

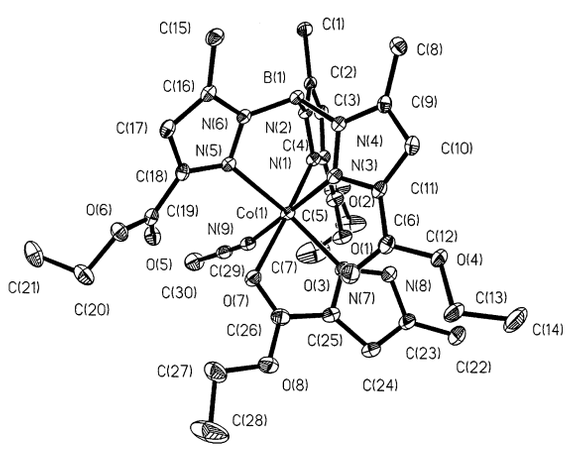

Fig. 2 Thermal ellipsoid diagram of [($Tp^{CO_2Et,Me}$)Co($pz^{CO_2Et,Me}$)-(ACN)]$^+$ (**3a**) with complete atomic labeling. The ellipsoids are drawn at the 20% probability level and hydrogen atoms have been removed for clarity.

and the ester carbonyl. The pyrazole N–H is stabilized *via* hydrogen bonding between one of the ester carbonyls of the Tp ligand and an oxygen of the perchlorate counterion. The lone remaining water has been replaced by an acetonitrile solvent molecule. The coordinated pyrazole must arise from decomposition of the $Tp^{CO_2Et,Me}$ ligand as there is no detectable free pyrazole in the starting material. Of course B–N bond cleavage in Tp ligands is not new, particularly for strongly Lewis acidic metals, thus it remains to be seen if hydrolytic chemistry derived from the bound water ligands is involved in this particular case.[9–11]

Electrospray mass spectrometry (ESI-MS) on this class of complex suggests that the ligands other than the Tp ester itself are relatively labile, as the only species observed under various instrumental conditions starting with $[Tp^{CO_2Et,Me}M(H_2O)_3]^+$, $[Tp^{CO_2Me,Me}Ni(Gly)(H_2O)]^+$, $[Tp^{CO_2Me,Me}Ni(MetOMe)(H_2O)]^+$, or $[Tp^{CO_2Et,Me}Co(pz^{CO_2Et,Me})ACN]^+$ is the $[Tp^{es}M]^+$ cation. Thus all *neutral* ligands, including the amino acids, pyrazole or water, are stripped away during the electrospray ionization process thereby severely limiting the utility of this method for characterization. However, it is notable that the transesterification process is easily followed by ESI-MS. Thus upon dissolving $[Tp^{CO_2Et,Me}M(H_2O)_3]^+$ (M = Co, Ni or Mn) in methanol and subjecting the mixture to ESI-MS analysis initially shows only masses corresponding to $[Tp^{CO_2Et,Me}M]^+$. There follows a gradual increase in a series of new mass peaks which are 14 mass units smaller than the parent. Thus for $[Tp^{CO_2Et,Me}Co(H_2O)_3]^+$, the initial isotopic mass cluster is centered at 530 amu and new isotopic clusters grow in at 516, 502 and 488 amu corresponding to the stepwise conversion of the Tp ligand from one having three ethyl esters groups to one with three methyl esters.

Reaction of base with metal-aquo complexes of Co, Ni, Mn, and Cu

While metal bound waters are potential nucleophiles, metal bound hydroxides are clearly much more powerful as such and are generally thought to be the active species involved in most hydrolytic metalloenzymes. Therefore we have looked to see if the metal bound waters in the aquo complexes could be deprotonated to yield metal hydroxo species. Unfortunately treatment of $[Tp^{CO_2Et,Me}M(H_2O)_3]^+$ where M = Ni, Co, or Mn with triethylamine in methanol/acetonitrile did not result in isolable metal hydroxo complexes but rather in the rearrangement product $[(Tp^{CO_2Me,Me})_2M]$. The structure of this class of complex is represented by $(Tp^{CO_2Me,Me})_2Ni$. In this case (Fig. 3, selected bond lengths and angles are collected in Table 1) two Tp ester ligands octahedrally encapsulate the Ni(II) cation to form a coordinatively saturated "sandwich" complex of a type well known for the sterically unencumbered trispyrazolylborates in general.[2] The formation of these structurally unremarkable complexes is driven in part by the reduced steric bulk that results from the conversion of the Tp ethyl ester ligand to the methyl ester *via* transesterification in methanol solution. Isomorphous and isostructural Co, and Mn complexes are also produced by this route but their structures are not reported here.

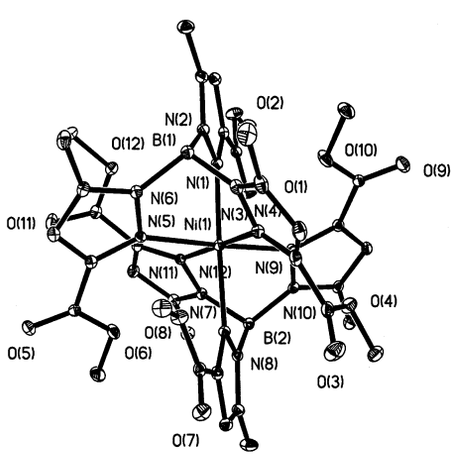

Fig. 3 Thermal ellipsoid diagram of $[(Tp^{CO_2Me,Me})_2Ni]$ (**4**) with partial atomic labeling (heteroatoms only). The ellipsoids are drawn at the 20% probability level and hydrogen atoms have been removed for clarity.

Table 2 Selected bond distances (Å) and angles (°) for $[Tp^{CO_2Et,Me}Cu(OH)]_2$ (**5**)[a]

Cu(1)–N(1)	2.069(8)	Cu(2)–N(9)	2.028(9)
Cu(1)–N(3)	2.401(8)	Cu(2)–N(11)	2.400(9)
Cu(1)–N(5)	2.014(9)	Cu(2)–O(13)	1.941(7)
Cu(1)–O(13)	1.926(7)	Cu(2)–O(14)	1.925(7)
Cu(1)–O(14)	1.925(8)	Cu(1)–Cu(2)	2.882(2)
Cu(2)–N(7)	2.086(8)		
N(1)–Cu(1)–N(3)	90.2(3)	N(7)–Cu(2)–N(11)	90.6(3)
N(1)–Cu(1)–N(5)	87.6(3)	N(7)–Cu(2)–O(13)	167.6(3)
N(1)–Cu(1)–O(13)	97.6(3)	N(7)–Cu(2)–O(14)	96.1(3)
N(1)–Cu(1)–O(14)	168.7(3)	N(9)–Cu(2)–N(11)	83.0(3)
N(3)–Cu(1)–N(5)	84.6(3)	N(9)–Cu(2)–O(13)	93.6(3)
N(3)–Cu(1)–O(13)	91.0(3)	N(9)–Cu(2)–O(14)	170.4(3)
N(3)–Cu(1)–O(14)	101.1(3)	N(11)–Cu(2)–O(13)	101.7(3)
N(5)–Cu(1)–O(13)	173.2(3)	N(11)–Cu(2)–O(14)	88.8(3)
N(5)–Cu(1)–O(14)	92.3(3)	O(13)–Cu(2)–O(14)	83.1(3)
O(13)–Cu(1)–O(14)	83.5(3)	Cu(1)–O(13)–Cu(2)	96.4(3)
N(7)–Cu(2)–N(9)	89.1(3)	Cu(1)–O(14)–Cu(2)	97.0(3)

[a] Numbers in parentheses are estimated standard deviations.

In solution, positive ion mode ESI-MS, reveals that the 1 : 1 $[TpM]^+$ cation is always the base peak observed but less intense peaks corresponding to the protonated 2 : 1 $[(Tp)_2MH]^+$ are also visible.

Treatment of the aquo complexes of Zn or Cu with triethylamine however did not follow the same pattern as that seen for Ni, Co and Mn(II). In these cases hydroxo bridged metal complexes could be isolated (the monohydroxo bridged Zn complex is reported in a separate publication).[12] The copper complex $[Tp^{CO_2Et,Me}Cu(OH)]_2$, **5** is shown in Fig. 4 (also see Table 2). It consists of a dihydroxo bridged dimer of $Tp^{CO_2Et,Me}$ where the copper atoms are pseudo-pentacoordinate with a square pyramidal geometry. Although the complex has near inversion symmetry it is not crystallographically imposed. The Cu–Cu distance of 2.883 Å is shorter than that seen with other similar dihydroxo bridged dimers including several trispyrazolyl-

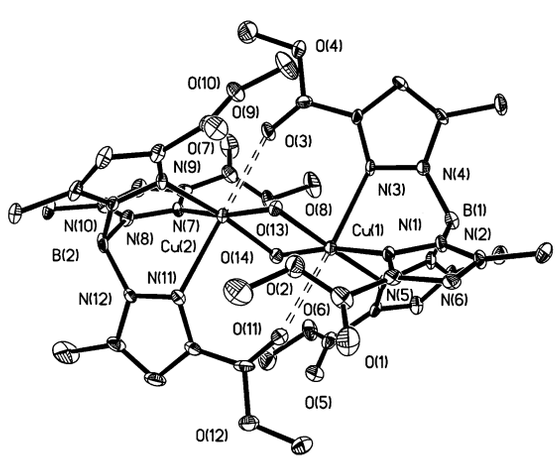

Fig. 4 Thermal ellipsoid diagram of $[Tp^{CO_2Et,Me}Cu(OH)]_2$ (**5**) with partial atomic labeling (heteroatoms only). The ellipsoids are drawn at the 20% probability level and the hydrogen atoms and the terminal methyl carbons of the ethyl esters have been removed for clarity. Dotted lines show the weak axial interaction between the ester carbonyl oxygens and the copper atoms.

borates, reported in the Cambridge Structural Database (CSD)[3] that range from 2.938–3.06 Å. This coupled with the more nearly regular $O_{hydroxide}$–Cu–$O_{hydroxide}$ angles, averaging 84°, leads to the largest $O_{hydroxide}$–$O_{hydroxide}$ separation of 2.591 Å (range in other Tp or triazacyclononane complexes 2.390–2.486Å). Although we have described the copper atoms in **5** as psuedo-pentacoordinate, they each show an additional rather long axial interaction with one of the ester carbonyl oxygens (Cu2–O3 2.674 Å and Cu1–O11 2.738 Å) so that the coordination geometry could also be described as strongly Jahn–Teller distorted octahedral.

When a solution of $[Tp^{CO_2Et,Me}Cu(H_2O)_2]^+$ is subject to ESI-MS, as with the other metal aquo complexes, only the $[Tp^{CO_2Et,Me}Cu]^+$ cation is observed. However, a solution of $Tp^{CO_2Et,Me}Cu(OH)_2CuTp^{CO_2Et,Me}$ shows isotopic peak clusters due to both $[Tp^{CO_2Et,Me}Cu]^+$ and $[Tp^{CO_2Et,Me}Cu(OH)H]^+$. Since neutral ligands appear not to be retained during the electrospray ionization process in other complexes of this type, we view the mass cluster representing $[Tp^{CO_2Et,Me}Cu(OH)H]^+$ as due to the presence in solution of the monomer $[Tp^{CO_2Et,Me}$-Cu(OH)] where the negatively charged hydroxide ion is retained but protonated. This suggests further that the dimeric structure seen in the solid state of **5** does not persist in solution although it does so in $[Tp^{CO_2Et,Me}Zn(OH)ZnTp^{CO_2Et,Me}]$.[12]

Reaction of Tp ester ligand with lanthanide ions

Although carbonyl oxygens without any formal negative charge are not in general good donors for metal ions, they are in fact predisposed to act as such in complexes where they are all pointed in toward the cavity. Evidence for weak interactions between these carbonyls and first row transition elements is seen in complexes **4** and **5** as well as in $[Tp^{CO_2Et,Me}Zn(OH)$-$ZnTp^{CO_2Et,Me}]$. However, in the presence of strong Lewis acid metals such as the lanthanides, a stronger interaction between the ester carbonyls and the metal is possible. Thus in $[(Tp^{CO_2Et,Me})_2La]ClO_4$, **6**, each Tp functions as a symmetrical η^6-N_3O_3 ligand for the lanthanum ion resulting in overall 12 coordination at the metal center (Fig. 5, Table 3). The La–N_{pz} bonds average 2.71(1) Å while the La–$O_{carbonyl}$ bonds are only slightly longer, 2.77(5) Å, giving pseudo-icosahedral symmetry around the La. These parameters differ from those seen with analogous lanthanide complexes of both pyridine substituted and secondary amide substituted Tp ligands.[13,14] In the former, each Tp functions as an η^6-N_3N_3' ligand to the lanthanide but the bonding is quite asymmetric with short bonds to the pyrazole nitrogens and longer ones to the pyridine nitrogens.[13] In the latter case one ligand adopts a symmetrical η^6-N_3O_3 mode of binding as seen here, while the second is η^4-N_2O_2 with a free uncoordinated arm, resulting in overall 10 coordinate

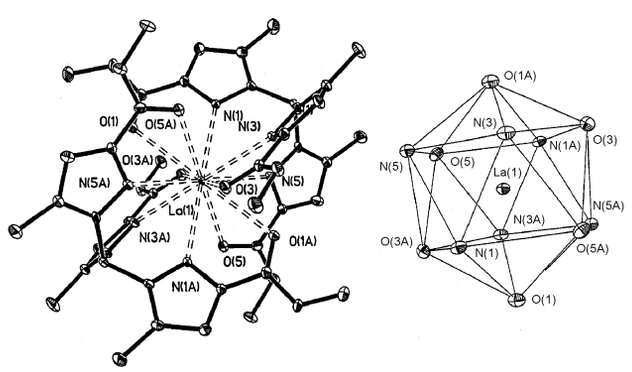

Fig. 5 Thermal ellipsoid diagram of $[(Tp^{CO_2Et,Me})_2La]^+$ (**6**) with partial atomic labeling (coordinating atoms only). The ellipsoids are drawn at the 20% probability level and the hydrogen atoms and the terminal methyl carbons of the ethyl esters have removed for clarity. The insert shows the near icosahedral symmetry around the La.

Table 3 Selected bond distances (Å) for $[(Tp^{CO_2Et,Me})_2La]ClO_4$ (**6**) and $[(Tp^{CO_2Me,Me})Gd(NO_3)_2]$ (**7**)[a]

	6	**7**
M(1)–N(1)	2.725(6)	2.546(5)
M(1)–N(3)	2.703(6)	2.470(5)
M(1)–N(5)	2.696(6)	2.528(5)
M(1)–O(1)	2.846(5)	2.552(5)
M(1)–O(3)	2.755(5)	2.584(5)
M(1)–O(5)	2.718(5)	2.567(5)
M(1)–O(7)		2.514(5)
M(1)–O(8)		2.479(5)
M(1)–O(10)		2.503(5)
M(1)–O(11)		2.471(2)

[a] Numbers in parentheses are estimated standard deviations.

metal.[14] The ^1H and ^{13}C NMR spectra support the notion that the symmetrical structure adopted by **6** in the solid state is maintained in solution.

A second type of lanthanide complex is represented by the "half-sandwich" $[(Tp^{CO_2Et,Me})Gd(NO_3)_2]$ **7**. In this case while only one Tp ester ligand is coordinated it adopts the same symmetrical η^6-N_3O_3 mode of binding seen in **6**. The remaining coordination sites are occupied by two symmetrical bidentate nitrate ions to give overall 10-coordination to the Gd (Fig. 6).

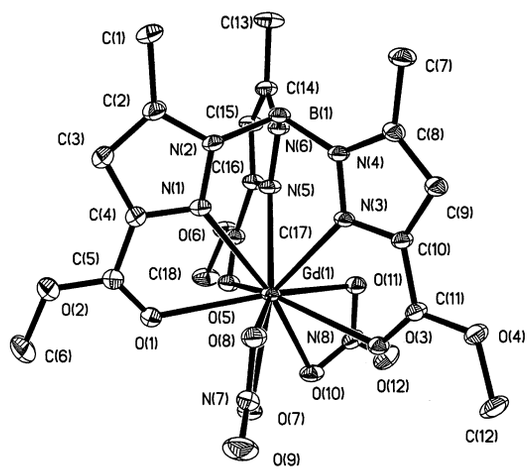

Fig. 6 Thermal ellipsoid diagram of $[(Tp^{CO_2Me,Me})Gd(NO_3)_2]$ (**7**) with complete atomic labeling. The ellipsoids are drawn at the 20% probability level and the hydrogen atoms have been removed for clarity.

The Gd–$O_{nitrate}$, Gd–N_{pz}, and Gd–O_{ester} bond lengths are all very similar (average 2.522(34) Å) in contrast to the strong asymmetry seen in the otherwise analogous lanthanide complexes of a pyridine substituted Tp ligand.[15] In the latter the M–N_{pz} bonds differ from the M–N_{py} bonds by over 0.2 Å. Again it is notable that only the methyl ester substituted ligand is isolated from reaction mixtures employing methanol as a solvent.

Infra-red spectroscopy

The various types of interactions that we have observed structurally with the Tp ester should also be reflected in the C=O stretching frequency of the ligand in the IR. Indeed the data show (Table 4) that the C=O stretching frequencies of the complexes structurally characterized thus far fall into three distinct groups: 1735–1720 cm^{-1} for completely non-interacting carbonyls, 1715–1700 cm^{-1} for carbonyls involved in H-bonding or weak complexation and 1690–1650 cm^{-1} for true coordination. In fact the groups are sufficiently well separated that different interactions between individual carbonyls can be observed in the same complex, as witnessed for $[Tp^{CO_2Et,Me}$-

Table 4 Carbonyl stretching frequencies in complexes of the ester substituted ligand $Tp^{CO_2R,Me}$

Compound	$\nu_{C=O}/cm^{-1}$ (KBr)	Interaction
$[(Tp^{CO_2Et,Me})ZnNO_3]$	1729	All uncoordinated
$[(Tp^{CO_2Et,Me})ZnOAc]$	1727, 1703	Uncoordinated and H-bonded
$[(NH_3Bu^t][(Tp^{CO_2Et,Me})]$	1714	All H-bonded
$[(Tp^{CO_2Me,Me})Ni(Gly)(H_2O)]^+$	1730, 1709, 1689	Uncoordinated/H-bonded/coordinated
$[(Tp^{CO_2Me,Me})Ni(MetOMe)H_2O)]^+$	1734, 1710, 1679	Uncoordinated/H-bonded/coordinated
$[(Tp^{CO_2Et,Me})Ni(H_2O)_3]^+$	1709	All H-bonded
$[(Tp^{CO_2Et,Me})Cu(H_2O)_2]^+$	1735, 1701	Uncoordinated and H-bonded
$[(Tp^{CO_2Et,Me})Co(H_2O)_3]^+$	1708	All H-bonded
$[(Tp^{CO_2Et,Me})Co(ACN)(pzH)]^+$	1728, 1710, 1669	Uncoordinated/H-bonded/coordinated
$[(Tp^{CO_2Et,Me})_2La]^+$	1681	All coordinated
$[(Tp^{CO_2Me,Me})_2Nd]^+$	1688	All coordinated
$[(Tp^{CO_2Me,Me})Gd(NO_3)_2]$	1678, 1666, 1651	All coordinated

$Co(ACN)(pz^{CO_2Et,Me})]^+$ which contains all three types of interactions. These correlations should be diagnostic indicators of the coordination mode of carbonyl containing Tp ligands like $Tp^{CO_2Et,Me}$ when crystal structures are unavailable. An interesting question is do the H-bonding interactions seen in the solid state persist in solution? The results for the complex $[Tp^{CO_2Et,Me}Co(H_2O)_3]^+$ are representative. In dichloromethane solution the infra-red spectra of $[Tp^{CO_2Et,Me}Co(H_2O)_3]^+$ is essentially identical to the solid state spectrum previously reported with relatively broad O–H stretching vibrations at 3450 and 3250 cm^{-1}, and a single sharp C=O stretch at 1710 cm^{-1} both indicative of coordinated water molecules H-bonded to the ester carbonyls as seen in the crystal structure. The spectrum in acetonitrile solution however is distinctly different in that a new relatively sharp feature becomes visible at 3624 cm^{-1} in the O–H region and a distinct shoulder at *ca.* 1730 cm^{-1} appears on the main the C=O stretching band at 1712 cm^{-1}. These changes suggest some loss of hydrogen bonding between the coordinated waters and the ester carbonyls with the concomitant appearance of features indicative of non-H-bonded water (*i.e.* both O–H and C=O stretching vibrations occur at higher frequency). More polar solvents could not be tested due to either low solubility or substitution for the coordinated water however the results in acetonitrile suggest that the internal H-bonding is relatively weak and would be completely lost in strong H-bonding solvents such as the alcohols or water.

Experimental

All syntheses were carried out in air and the reagents and solvents purchased from commercial sources and used as received unless otherwise noted. Methanol was distilled under argon over CaH_2. Potassium tris(3-carboxyethyl-5-methyl)-pyrazolylborate and $[Tp^{CO_2Et,Me}M(H_2O)_3]^+$ where M = Ni, Co, Mn, or Cu(II) were prepared using the previously reported procedures.[7]

Synthesis

$[Tp^{CO_2Me,Me}Ni(MetOMe)(H_2O)]ClO_4$ (1). To a solution of 0.208 g $[Tp^{CO_2Et,Me}Ni(H_2O)_3]ClO_4$ (0.3 mmol) in methanol, was added 0.061 g of methionine methyl ester (0.3 mmol) and 0.061 g of triethylamine (0.6 mmol). The mixture was stirred for 2 h before being concentrated under vacuum. Crystallization of the crude product was from methanol–ether. Anal. calc. (found) for $[Tp^{CO_2Me,Me}Ni(MetOMe)(H_2O)]ClO_4\cdot CH_3OH$ ($C_{24}H_{39}O_{14}N_7BSClNi$): C, 36.65 (36.88); H, 4.99(4.38); N, 12.46 (12.23)%. FTIR (KBr/cm^{-1}): ν = 2576 (B–H), 1734, 1679 (C=O). λ_{max}/nm (CH_3CN, ε/M^{-1} cm^{-1}): 378 (30), 614 (10).

$[Tp^{CO_2Me,Me}Ni(Gly)(H_2O)]ClO_4$ (2). To a solution of 0.122 g $[Tp^{CO_2Et,Me}Ni(H_2O)_3]ClO_4$ (0.18 mmol) in acetonitrile–methanol was added 0.014 g of glycine and 0.018 g of triethylamine (0.18 mmol). The reaction mixture was stirred for 5 h and concentrated under vacuum. Slow diffusion of ether into the concentrated solution produced analytically pure crystals. Anal. calc. (found) for $[Tp^{CO_2Me,Me}Ni(Gly)(H_2O)]ClO_4\cdot CH_3CN\cdot C_2H_5OC_2H_5$, ($C_{26}H_{41}O_{14}N_8BClNi$): C, 39.27 (40.23); H, 5.20 (5.49); N, 14.10 (14.29)%. FTIR (KBr/cm^{-1}): ν = 2569 (B–H), 1730, 1689 (C=O). λ_{max}/nm (CH_3CN, ε/M^{-1} cm^{-1}): 374 (35), 618 (10).

$[(Tp^{CO_2Et,Me})Co(pz^{CO_2Et,Me})(solv)]ClO_4$ (3). An acetonitrile–ether solution of $[(Tp^{CO_2Et,Me})Co(H_2O)_3]ClO_4$ was allowed to stand several weeks in a closed tube at room temperature. The pink crystals that subsequently appeared were determined by X-ray diffraction to be that of $[(Tp^{CO_2Et,Me})Co(pz^{CO_2Et,Me})(ACN)]ClO_4$, **3a**. Filtration of the solid followed by washing with ether and air-drying caused the crystals to collapse. The bulk material was shown by elemental analysis to be the aquo complex $[(Tp^{CO_2Et,Me})Co(pz^{CO_2Et,Me})(H_2O)]ClO_4$, **3b**. Compound **3b** can also be produced in a rational route by the addition of 3-carboxyethyl-5-methylpyrazole to an acetonitrile solution of $[(Tp^{CO_2Et,Me})Co(H_2O)_3]ClO_4$. Anal. calc. (found) for $[(Tp^{CO_2Et,Me})Co(pz^{CO_2Et,Me})(H_2O)]ClO_4\cdot H_2O$, ($C_{28}H_{42}N_8O_{14}BClCo$): C, 41.02 (40.82); H, 5.16 (5.02); N, 13.67 (13.52)%. FTIR (KBr/cm^{-1}): ν = 2565 (B–H), 1727 (C=O), 1710 (C=O), 1669 ($C=O_{pz}$). λ_{max}/nm (CH_3CN, ε/M^{-1} cm^{-1}): 500 (28). Magnetism (solid state, room temperature): μ_{eff} = 4.6 μ_B.

$[(Tp^{CO_2Me,Me})_2Ni]$ (4). A solution of $[Tp^{CO_2Et,Me}Ni(H_2O)_3]ClO_4$ in acetonitrile–methanol was treated with 1 equivalent of Et_3N. Crystallization by slow diffusion of ether into the concentrated solution gave the sparingly soluble product. Anal. calc. (found) for $[(Tp^{CO_2Me,Me})_2Ni]$ ($C_{36}H_{44}O_{12}N_{12}B_2Ni$): C, 47.15 (46.92); H, 4.84 (4.48); N, 18.34 (18.12)%. FTIR (KBr/cm^{-1}): ν = 2564 (B–H), 1752, 1708 (C=O). λ_{max}/nm (CH_3CN, ε/M^{-1} cm^{-1}): 368 (20), 614 (10). The analogous Co(II) and Mn(II) complexes **4b** and **4c** were prepared in the same way.

$[Tp^{CO_2Et,Me}Cu(OH)_2CuTp^{CO_2Et,Me}]$ (5). A solution of $[Tp^{CO_2Et,Me}Cu(H_2O)_3]ClO_4$ in methanol was treated with 1 equivalent of Et_3N and stirred for 6 h. The green solid was filtered off. Crystals suitable for X-ray diffraction were grown by slow diffusion of hexane into a CH_2Cl_2 solution of **5**. Although the X-ray crystal structure revealed that the ligand was exclusively in the form of its ethyl ester, the bulk material analyzed as a 1 : 1 mixture of the methyl and ethyl esters. Anal. calc. (found) for $Tp^{CO_2R,Me}Cu(OH)_2CuTp^{CO_2R,Me}$, ($C_{39}H_{52}O_{14}N_{12}B_2Cu_2$): C, 44.12 (43.70); H, 4.94 (4.85); N, 15.83 (15.84)%. FTIR (KBr/cm^{-1}): ν = 2536 (B–H), 1727 (C=O). λ_{max}/nm (CH_3CN, ε/M^{-1} cm^{-1}): 628 (50).

$[(Tp^{CO_2Et,Me})_2La]ClO_4$ (6). A slurry of potassium tris(3-carboxyethyl-5-methyl)pyrazolylborate (0.31 g, 0.60 mmol) in 30 ml of CH_3OH was treated dropwise with a methanol solution of $La(ClO_4)_3\cdot 6H_2O$ (0.33 g, 0.60 mmol). The resulting solution was warmed to 60 °C, stirred for 24 h, and filtered. The

Table 5 Summary of crystallographic data and parameters for $[Tp^{CO_2Me,Me}Ni(Gly)(H_2O)]ClO_4$ (**2**), $[(Tp^{CO_2Et,Me})Co(pz^{CO_2Et,Me})(ACN)]ClO_4$ (**3**), $[(Tp^{CO_2Me,Me})_2Ni]\cdot ACN$ (**4**), $[(Tp^{CO_2Et,Me})Cu(OH)]_2$ (**5**), $[(Tp^{CO_2Et,Me})_2La]ClO_4$ (**6**), and $[(Tp^{CO_2Me,Me})Gd](NO_3)_2$ (**7**)

	2	**3**	**4**	**5**	**6**	**7**
Molecular formula	$C_{26}H_{41}BClN_8O_{14}Ni$	$C_{30}H_{41}BClN_9O_{12}Co$	$C_{38}H_{47}B_2N_{13}O_{12}Ni$	$C_{42}H_{51}B_2N_{12}O_{14}Cu_2$	$C_{42}H_{56}B_2ClN_{12}O_{16}La$	$C_{18}H_{22}BN_8O_{14}Gd$
FW	794.64	824.40	957.82	1096.65	1181.0	742.50
T/K	293(2)	153(2)	293(2)	153(2)	203(2)	293(2)
Crystal system	Triclinic	Triclinic	Monoclinic	Trigonal	Triclinic	Triclinic
Space group	$P\bar{1}$	$P\bar{1}$	$P2_1/n$	$P3_12_1$	$P\bar{1}$	$P\bar{1}$
a/Å	11.155(2)	10.6010(3)	19.325(4)	12.020(2)	9.931(2)	9.735(2)
b/Å	12.759(4)	12.1127(5)	11.299(2)	12.020(2)	11.477(4)	12.401(3)
c/Å	15.321(3)	16.2410(5)	19.940(4)	57.228(11)	12.852(2)	15.351(2)
α/°	93.89(2)	72.232(2)	90	90	72.04(3)	106.92(8)
β/°	109.95(1)	75.474(2)	92.51(3)	90	88.00(3)	90.50(2)
γ/°	107.12(2)	72.263(2)	90	120	73.80(4)	105.36(2)
Z	2	2	4	6	1	2
V/Å^3	1924.2(8)	1862.71(11)	4350(2)	7161(2)	1336.0(6)	1702.3(6)
μ_{calc}/mm^{-1}	0.643	0.605	0.523	0.970	0.925	2.014
F(000)	830	857	1988	3402	604	734
Crystal dimensions/mm	0.4 × 0.4 × 0.5	0.015 × 0.05 × 0.08	0.1 × 0.2 × 0.4	0.2 × 0.2 × 0.2	0.5 × 0.5 × 0.4	0.6 × 0.6 × 0.5
Radiation	Mo-Kα (λ = 0.71073 Å)	Mo-Kα (λ = 0.71073 Å)	Mo-Kα (λ = 0.71073 Å)	Mo-Kα (λ = 0.71073 Å)	Mo-Kα (λ = 0.71073 Å)	Mo-Kα (λ = 0.71073 Å)
No. of reflections collected	5322	31855	17148	11009	3493	6272
No. of unique reflections	5017	8353	9944	6978	3247	5891
No. of parameters	478	514	595	669	355	379
Refinement method	Full-matrix least-squares on F^2	Full-matrix least-squares on F^2	Full-matrix least-squares on F^2	Full-matrix least-squares on F^2	Full-matrix least-squares on F^2	Full-matrix least-squares on F^2
$R(F)$ [a]	0.0670	0.0572	0.0549	0.0828	0.0588	0.0430
$R_w(F^2)$ [b]	0.1521	0.1476	0.1298	0.1393	0.1525	0.1415

[a] $R = [\Sigma|\Delta F|/\Sigma|F_o|]$. [b] $R_w = [\Sigma\, w(\Delta F)^2/\Sigma\, wF_o^2]$. [c] Goodness of fit on F^2.

filtrate was concentrated under reduced pressure and allowed to slowly evaporate on the bench top to give 0.18 g (25%) of $[(Tp^{CO_2Et,Me})_2La]ClO_4$ as light yellow blocks. A similar Nd complex **6b** prepared from the metal nitrate in methanol was isolated as the Tp methyl ester complex $[(Tp^{CO_2Me,Me})_2Nd]NO_3$ and characterized by X-ray crystallography (data not shown). Anal. calc. (found) for $[(Tp^{CO_2Et,Me})_2La]ClO_4 \cdot H_2O$ ($C_{42}H_{58}N_{12}O_{17}B_2ClLa$): C, 42.07 (41.69); H, 4.89 (4.52); N, 14.02 (14.03)%. ^{1}H NMR ($CDCl_3$) δ 6.27 (s, 1 H, Pz*H*), 3.74 (q, 2 H, J = 7 Hz, –OCH_2–), 2.58 (s, 3 H, Pz-CH_3), 0.98 (t, 3 H, J = 7 Hz, –CH_3). ^{13}C NMR ($CDCl_3$) δ 166.06, 144.20, 142.27, 105.17, 61.66, 13.95, 12.84. FTIR (KBr/cm^{-1}): ν = 2542 (B–H), 1681 (C=O).

$[(Tp^{CO_2Me,Me})Gd](NO_3)_2$ (7). A 100 ml round bottom flask was charged with 319.3 mg (0.626 mmol) of potassium tris(3-carboxyethyl-5-methyl)pyrazolylborate and 30 ml of methanol. To this turbid solution was added 282.3 mg (0.625 mmol) of $Gd(NO_3)_3 \cdot 6H_2O$ in 20 ml of methanol. The clear solution was left to stir for three hours. The solvent was removed, the residue redissolved in dichloromethane (20 ml), and then filtered. The pale yellow colored filtrate was reduced to a volume of about 10 ml, upon which hexane (8 ml) was carefully layered. The solution was left at −20 °C whereupon fragile, colorless rods, suitable for diffraction studies deposited over a period of six days. The rod-like crystals are solvent-sensitive, readily powdering when dried. Total yield was 282 mg (60%). Anal. calc. (found) for $[(Tp^{CO_2Me,Me})Gd(NO_3)_2] \cdot 0.33C_6H_{14}$ ($C_{21}H_{26.6}N_8BO_{12}Gd$), C, 32.42 (32.19); H, 3.63 (3.48); N, 15.19 (14.70)%. FTIR (KBr/cm^{-1}): ν = 2562 (B–H), 1678, 1666, 1651 (C=O).

Physical methods

Elemental analyses were obtained from Quantitative Technologies, Inc., Whitehouse, NJ. All samples were dried *in vacuo* prior to analysis. The presence of solvates was corroborated by FTIR, ^{1}H NMR, or X-ray crystallography. ^{1}H and ^{13}C NMR spectra were collected on a Varian UNITY INOVA 400 MHz NMR spectrometer. Chemical shifts are reported in ppm relative to an internal standard of TMS. The ^{13}C quaternary carbon peaks that are not observed are a result of either poor solubility and/or overlapping signals. Electrospray mass spectra (ESI-MS) were recorded on a Finnigan LCQ ion-trap mass spectrometer equipped with an ESI source (Finnigan MAT, San Jose, CA). A gateway PC with Navigator software version 1.2 (Finnigan Corp., 1995–1997), was used for data acquisition and plotting. Isotope distribution patterns were simulated using the program IsoPro 3.0 (MS/MS Software, Sunnyvale, CA). IR spectra were recorded as KBr disks or in solution on a Perkin-Elmer Spectrum One FTIR spectrometer equipped with a Dell Optiplex PC. Electronic spectra were recorded using a Hewlett-Packard 8452A diode array spectrophotometer.

X-Ray crystallography

Crystal, data collection, and refinement parameters for **2**–**7** are given in Table 5. Crystals of all complexes were sealed in thin-walled quartz capillaries, mounted on either a Siemens P4 diffractometer with a sealed-tube Mo X-ray source (λ = 0.71073 Å) controlled *via* a PC (data collected at 293 K) or a Nonius Kappa CCD diffractometer (data collected at 153 K). For the Siemens system automatic searching (Siemens XSCANS 2.1), centering, indexing, and least-squares routines were carried out for each crystal with at least 25 reflections in the range, $20 \leq 2\theta \leq 25°$ used to determine the unit cell parameters. During the data collection, the intensities of three representative reflections were measured every 97 reflections, and any decay observed was empirically corrected for by the software during data processing. We thank Dr Vincent Lynch, Department of Chemistry University of Texas at Austin for data collection on the CCD diffractometer. The structures were all solved using direct methods or *via* the Patterson function, completed by subsequent difference Fourier syntheses, and refined by full-matrix least-squares procedures on F^2. All non-hydrogen atoms were refined with anisotropic displacement coefficients with hydrogens treated as idealized contributions using a riding model except were noted. All software and sources of the scattering factors are contained in the SHELXTL 5.0 program library (G. M. Sheldrick, Siemens XRD, Madison, WI). Selected bond distances and angles for these complexes are shown in Tables 1–3.

CCDC reference numbers 159086, 159091 and 186437–186440.

See http://www.rsc.org/suppdata/dt/b2/b204277k/ for crystallographic data in CIF or other electronic format.

Acknowledgements

This work was supported in part by Grants AI-1157 from the Robert A. Welch Foundation and CHE-9726488 from the NSF. The NSF-ILI program grant USE-9151286 is acknowledged for partial support of the X-ray diffraction facilities at Southwest Texas State University. We thank Dr Vincent Lynch, Department of Chemistry, University of Texas at Austin for the data collection of **3**–**5** on the Nonius Kappa CCD diffractometer.

References

1 N. Armstrong, *Biochemistry*, 2000, **39**, 13625.
2 October 2001 release version 5. 22 Cambridge Structural Data Base, Cambridge Crystallographic Data Center, Cambridge, UK, 2001.
3 S. Trofimenko, *Scorpionates: The Coordination Chemistry of Polypyrazolylborate Ligands*, Imperial College Press, London, UK, 1999.
4 N. Kitajima, K. Fujisawa, C. Fujimoto, Y. Moro-oka, S. Hashimoto, T. Kitagawa, K. Toriumi, K. Tatsumi and A. Nakamura, *J. Am. Chem. Soc.*, 1992, **114**, 1277.
5 N. Kitajima, K. Fujisawa, M. Tanaka and Y. Moro-oka, *J. Am. Chem. Soc.*, 1992, **114**, 9232.
6 A. Looney, S. Trofimenko, G. Parkin, R. Alsfasser, M. Ruf and H. Vahrenkamp, *Inorg. Chem.*, 1991, **30**, 4098.
7 S. M. Carrier, C. E. Ruggiero and W. B. Tolman, *J. Am. Chem. Soc.*, 1992, **114**, 4407.
8 B. S. Hammes, M. W. Carrano and C. J. Carrano, *J. Chem. Soc., Dalton Trans.*, 2001, 1448.
9 E. Kime-Hunt, K. Spartalian, M. DeRusha, C. M. Nunn and C. J. Carrano, *Inorg. Chem.*, 1989, **28**, 4392.
10 D. C. Bradley, M. B. Hursthouse, J. Newton and N. P. Walker, *J. Chem. Soc., Chem. Commun.*, 1984, 188.
11 D. L. Hughes, G. J. Leigh and D. G. Walker, *J. Chem. Soc., Dalton Trans.*, 1988, 1153.
12 B. S. Hammes, X. Liu, M. W. Carrano and C. J. Carrano, *Inorg. Chim. Acta*, 2002, in press.
13 R. L. Paul, A. J. Amoroso, P. L. Jones, S. M. Couchman, Z. R. Reeves, L. H. Rees, J. C. Jeffery, J. A. McCleverty and M. D. Ward, *J. Chem. Soc., Dalton Trans.*, 1999, 1563.
14 A. L. Rheingold, C. D. Incarvito and S. Trofimenko, *J. Chem. Soc., Dalton Trans.*, 2000, 1233.
15 P. L. Jones, A. J. Amoroso, J. C. Jeffery, J. A. McCleverty, E. Psillakis, L. H. Rees and M. D. Ward, *Inorg. Chem.*, 1997, **36**, 10.